

FATIGUE LIFE ASSESSMENT OF THE IS28B2 SAILPLANE

by James M. Ritchie, A.O. Payne and Prof. N. Mileschkin, Royal Melbourne Institute of Technology, Australia

Presented at the XXIV OSTIV Congress, Omarama, New Zealand (1995)

Summary

This paper gives an account of a life extension program carried out for the Gliding Club of Victoria (GCV) on the IS28B2 sailplane manufactured by the Intreprinderea De Constructii Aeronautice Brasov, Romania. The GCV, based at Benalla in the North East of Victoria, Australia, have operated six IS28B2s for 15 years amassing a total of over 35,000 hours flying time and have found them excellently suited to their training operations. They therefore engaged the Royal Melbourne Institute of Technology to undertake a comprehensive fatigue investigation to extend the life originally determined by the manufacturer. The first phase was a program to extend the safe fatigue life, followed by a second phase, which is still in progress, to develop a safety-by-inspection procedure to extend the life still further by conducting regular inspections at calculated intervals.

1. Introduction

Early fatigue substantiation of the IS28B2 design was conducted by the manufacturer with a two load level fatigue test on a centre wing and fuselage using a locally derived load spectrum. The test was stopped at a life under the spectrum of 250,000 hours (unfactored) and examination of the structure found no evidence of cracking.

Applying the most severe Australian sailplane spectrum available at that time, the manufacturer transposed the fatigue life and subsequently placed a safe life of 10,000 flying hours or 30,000 landings on the IS28B2.

The Gliding Club of Victoria (GCV) operate six IS28B2s for ab-initio and advanced pilot training. Several of the fleet have exceeded the manufacturer's recommended safe life and are at the time of writing operating on a safety by inspection basis until 14,000 flight hours or 42,000 landings.

The GCV are interested in keeping their IS28B2s for

primary training and hence initiated and funded this further study into fatigue substantiation of the sailplane.

2. Sailplane Description

2.1 General Characteristics

The IS28B2 is of conventional design as shown in Figure 1. The wings are single spar, all aluminum alloy structure joined on the centre-line by high tensile steel lugs. Fuselage primary structure is aluminum alloy with

glass fibre fairings around the wing to fuselage junction and the nose cone. The tailplane is also aluminum alloy with glass fibre fairings at the tail attachment. All surface skins are metal except for aileron, elevator and rudder surfaces which are fabric covered. Principal dimensions are presented in Table 1.

2.2 Fatigue Critical Areas
Following a tear-down inspection of un-serviceable

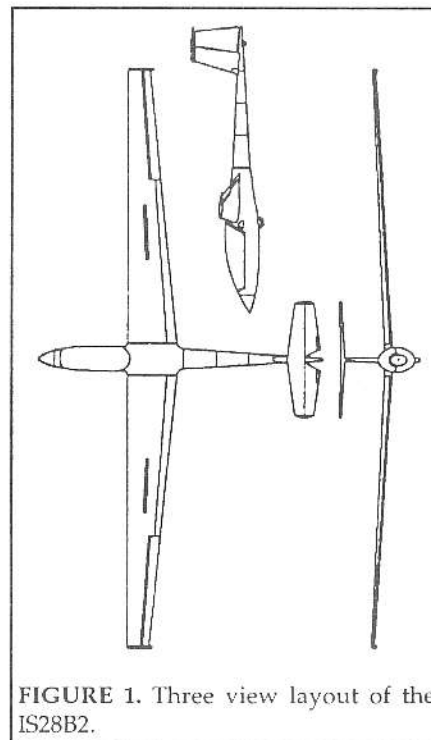


FIGURE 1. Three view layout of the IS28B2.

TABLE 1
Characteristics of the IS28B2

Wing Area (m^2)	18.24
Wing Span (m)	17
Aspect Ratio	15.8
Mean Aerodynamic Chord (m)	1.13
Root Chord, Tip Chord (m)	1.46, 0.65
Incidence, Dihedral (deg)	4, 2.5
Quarter Chord Sweep (deg)	2.0
Horizontal Tail Area (m^2),	2.73
Horizontal Tail Span (m)	3.48
Vertical Tail Area (m^2)	1.5
Vertical Tail Span (m)	1.5
Wing Flap Span (m)	4.5

structures, examination of construction drawings and previous engineering studies, eight fatigue critical regions were identified and subjected to a detailed fatigue analysis.

Figure 2 shows critical Area 1, Area 2 and Area 3 located on the wing main spar inboard of the root rib. The wing centre lug is clamped between two parts of the spar flange using steel bolts. The carry-through spar at the root rib is highly loaded since primary bending loads outboard of the root rib must be channelled into this member, and the forward sweep of the spar creates differential bending that adds tension to the rear side of the lower flange under normal flight conditions.

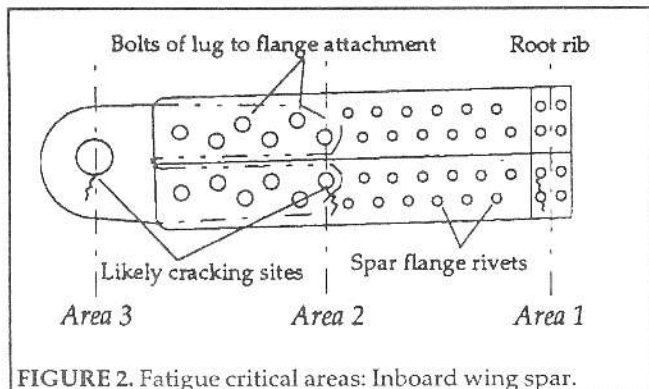


FIGURE 2. Fatigue critical areas: Inboard wing spar.

Cracking may initiate from rivet holes where the root rib and spar are fastened, from bolt holes at the spar to lug joint and from the alloy steel lug.

Figure 3 shows location Area 4 outboard of the wing root where the forward flange component of the main spar terminates. Local stress concentration may lead to cracking from rivet holes in the spar flange.

The horizontal tail is a conventional spar, rib and skin structure. Built-up structure outboard of the centre attach-

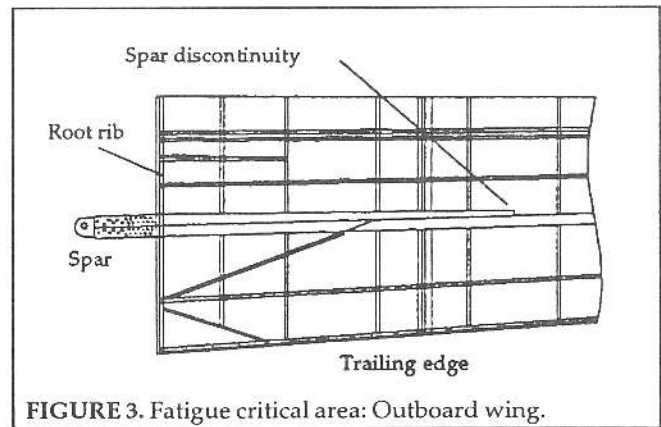


FIGURE 3. Fatigue critical area: Outboard wing.

ment has low stresses, but the skin and spar flanges end at the root rib, causing a considerable change in the load path and hence an increase in stress at the joint of left and right tailplanes. Fluctuating tensile stresses in the spar's top edge and through the net section of the top centre lugs make those areas susceptible to fatigue; shown in Figure 4 as Area 5 and Area 6.

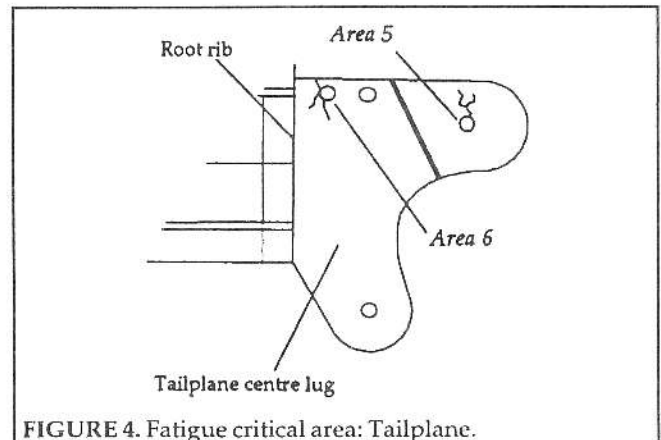


FIGURE 4. Fatigue critical area: Tailplane.

A primary non-redundant component of the wing to fuselage mating is the fuselage spigot, shown in Figure 5. The spigots are intractable to accurate stress analysis and so fatigue calculations have been done on a conservative basis, for possible cracking through the minimum cross-section adjacent to the spigot collar. This location was designated Area 7.

The possibility of fatigue in the vertical tail (Area 8) is accentuated by cracking discovered in a fuselage bulkhead riveted to the forward fin spar. Significant in-flight stresses arise since the horizontal tail has dihedral, and any

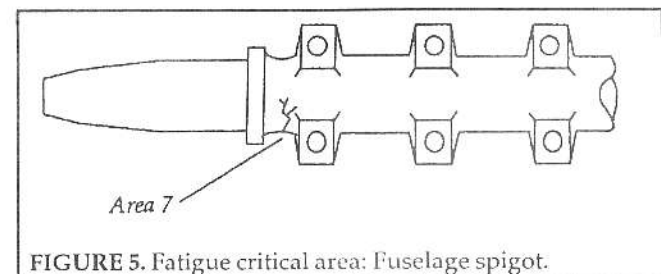


FIGURE 5. Fatigue critical area: Fuselage spigot.

bending on the fin is enhanced during yaw by the rolling moment of the horizontal tail. This part of the airframe is also exposed to stresses from ground towing using the tail dolly and impact forces on landing from the unsprung tail wheel which are believed to have initiated the cracks discovered.

3. Mission Profile

3.1 Division of Roles

To establish the frequency of all prescribed roles and maneuvers a short survey form was incorporated into the normal days flying that questioned the pilot on factors relevant to their flight. The survey recognised individual aircraft, allowing a specific breakdown for each of the six sailplanes to be obtained. The survey ran for one year, from May 1991, to May 1992 and the results are shown in Table 2.

TABLE 2
Breakdown of GCV Roles

Aircraft	Training (all maneuvers)		Private Hire (all maneuvers)	
	Dual %	Solo %	Dual %	Solo %
GVZ	68.97	2.19	21.43	7.41
GVW	66.10	3.14	25.29	5.47
CQF	69.17	3.34	20.42	7.07
GII	77.34	6.44	11.65	4.57
WVV	72.68	6.05	15.42	5.85
CVY	82.64	4.57	7.85	4.94
Average	72.81 %	4.29 %	17.01 %	5.89 %

Average flight times are very consistent in recent years and vary little from the mid 1970s when the fleet entered service. The average flight time for this study was taken as 18 minutes and that leads to just over 3 landings per flight hour.

3.2 Load Spectra

An analysis of a typical flight strain record was made to obtain equivalent load cycle counts by the Range Mean Pair Count and the Maximum Peak to Minimum Trough Count methods that are widely used in the aircraft fatigue field. Typical fatigue data were then used to carry out a life estimation for the two cycle counting methods (in effect for three cycle counting techniques because the Rainflow and Range Mean Pair methods converge for a long sequence). These results for flight loads have then been compared with a life estimate from a Fatigue Meter Count using the same fatigue data and all methods give lives which agree closely. It is concluded that for the fatigue sequence here at least, the Fatigue Meter Count gives a valid estimate of life.

Initially, three fatigue meters were installed in IS28B2s to record the frequencies of centre of gravity accelerations. Periods of measurement over 50 hours were taken to ensure a broad cross-section of pilots. One measured spectrum encompassed GCV operations with no aerobatics other than the compulsory spin training conducted by the GCV and a second spectrum was

measured that did include aerobatics. The aerobatic spectrum is compared with other spectra for sailplanes operated in Australia (Figure 6 and Figure 7), which include significant data from cross-country and aerobatic roles in glass fibre and metal sailplanes. The Dorning spectrum represents an upper envelope of all Australian data.

The measured IS28B2 aerobatic spectra are indicative of present day GCV operations, and are considered to represent the sailplanes history suitably.

4. Theoretical Studies

To complement experimental strain measurements a theoretical study was made into stress distribution at identified fatigue critical areas.

Lifting Line theory was used to determine lift distributions over the sailplane wing for various configurations and speeds. To determine tailplane loads for balanced flight, the lift, drag and pitching properties of wings, fuselage and tailplane were estimated. A summation of subsequent moments about the sailplane CG allowed the derivation of balance loads. Lastly, Engineers' Bending theory was used to calculate the bending stresses within the wing and tailplane structure. The maximum stresses, occurring at the outermost fibres on the spar section, were considered. Figure 8 shows the calculated extreme glass fibre stresses for the wing spar in a clean configuration, operating at a lift coefficient of unity.

The theoretical analysis gave good comparisons with strain measurements on the critical inner wing spar for normal flight configurations (excluding the effects of flap and dive-brake).

5. In-flight Data Acquisition

In-flight parameters measured in the IS28B2 were strains

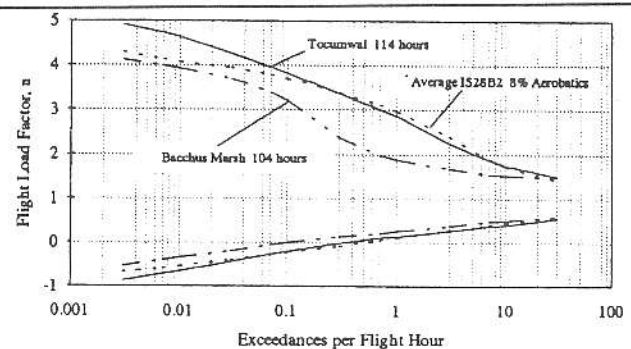


FIGURE 6. Blanik flight spectra and IS28B2 spectrum.

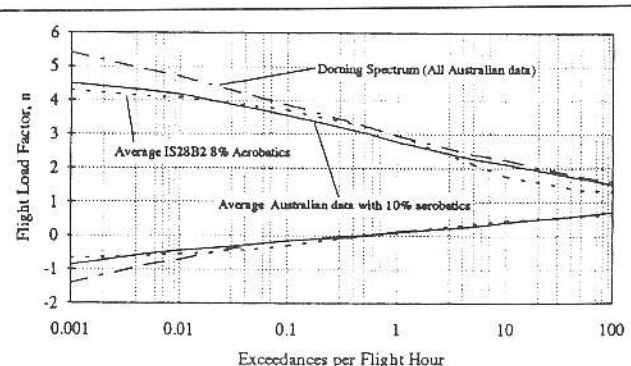


FIGURE 7. Dorning spectrum, average Australian data and IS28B2 spectrum.

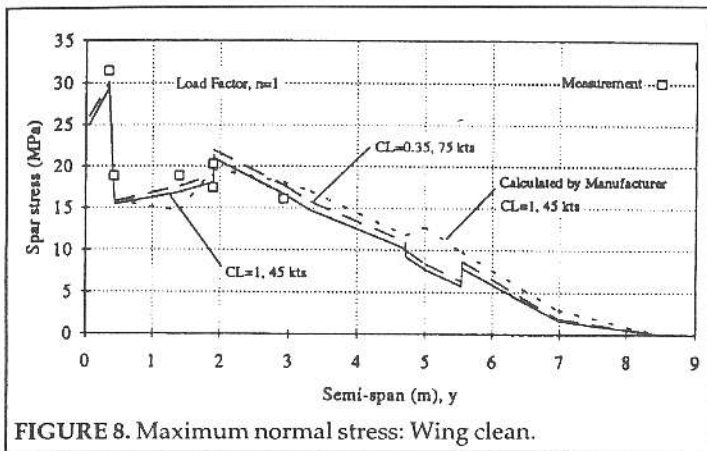


FIGURE 8. Maximum normal stress: Wing clean.

in the identified critical areas, indicated airspeed and the center of gravity vertical acceleration. This enabled the strain per g at critical locations on the airframe for different maneuvers and sailplane configurations to be determined. A general layout of the instrumentation used is shown in Figure 9.

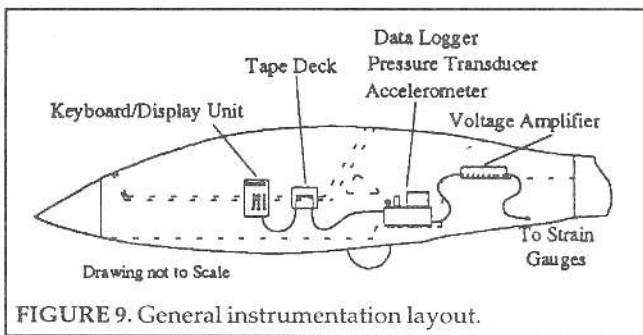


FIGURE 9. General instrumentation layout.

In total 24 ersg's were used on the IS28B2 airframe. The wing main spar had 18 gauges between the root region and dive-brake; the horizontal tailplane had 4 gauges at the root attachment, and the remaining two were attached to the forward fin spar. Figure 10 shows strain gauge stations on the wing spar; for clarity the outermost gauges at station 2830 mm have been excluded.

Recorded strains were plotted against CG acceleration

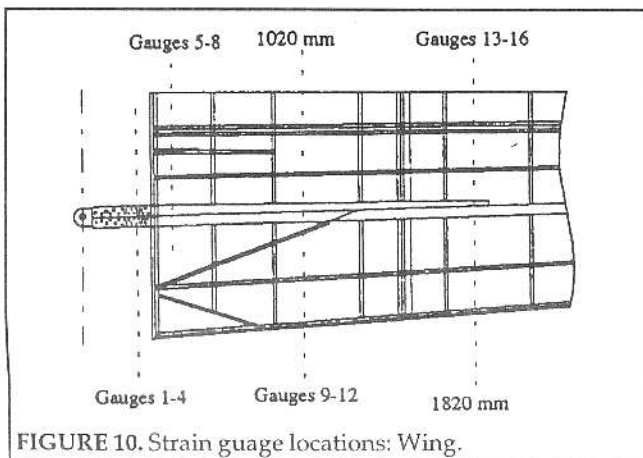


FIGURE 10. Strain gauge locations: Wing.

and a method of *least squares* curve fit was used to obtain a linear strain per g relationship. The correlation coefficient was the primary indicator for goodness of fit. Generally the correlation between strain and g was considered strong for coefficients > 0.75.

A typical plot of load factor against stress is shown in Figure 11. The recording was taken at the root rib on the lower rear flange. To determine the change in stress per g with take-off weight, flights were made with several different pilots of known weight and a short recording of stress made from straight and level flight to give the 1 g stress condition.

The average measurement from all gauges at a particular wing station (as shown in Figure 10) are given in Table 3.

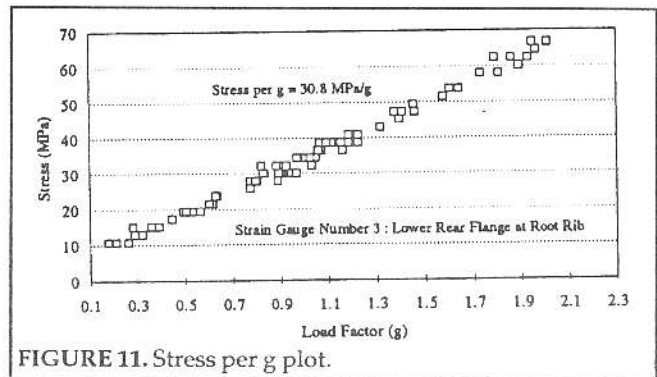


FIGURE 11. Stress per g plot.

TABLE 3
Measured Stress per g: Wing gauges.

Gauge Numbers	Measured Stress /g, (MPa/g)			
	Dual Normal Flight	Dual Low Tow Flap 5 deg	Dual Flap 15deg	Solo Normal Flight
1 to 4	28.47	27.69	22.83	21.48
5 to 8	17.08	15.99	13.00	12.90
9 to 12	16.15	14.19	12.73	
13 to 16	12.95	11.45	10.85	
17 and 18	14.65	14.00	10.70	

6. Fatigue Life Estimation

6.1 Fatigue Data

For those areas of the wing subjected to the fatigue test it is only necessary to transpose the life reached under the test loading, to the life that would be reached under the measured service loading. To do this, representative fatigue data for critical regions of the wing have been taken and adjusted by linear multiplication of fatigue life to predict failure at 250,000 hours of the test loading. For aluminum alloy components for which the S-N curves are linear or close to linear on a $\log_{10}S - \log_{10}N$ basis this would be exact if the S-N curves have the right slope.

In the case of the wing spar steel lug the lower load of the spectrum was found to be very close to the fatigue limit of the relevant S-N curve and this has therefore been adjusted by linear multiplication of stress.

The ESDU Data Sheet E.02.01 giving endurance curves

for complete wing and tailplane structures were applied to the fatigue critical areas of the wing root, outboard wing spar discontinuity and tailplane. Additionally notched aluminum alloy curves (5), with an appropriately calculated stress concentration factor, were applied to the wing spar at the root rib. Specific fatigue data, as published by the ESDU data sheets, for steel lugs and bolted joints were applied in the appropriate areas on the inner wing (Area 2 and 3). Similarly, ESDU Data Sheet E.05.01 was applied for the lug to spar joint and E.05.05 for the lug itself.

Conservative calculations of stress in the steel spigot at the collar and in the bolt holes attaching the assembly to the fuselage were made and reference to the Mil Handbook for high strength steels, of appropriate UTS, showed that the highest stress in the spectrum was below the fatigue limit.

For areas of the structure not subjected to fatigue testing (outer wing and tailplane), the predicted fatigue life is taken without any factoring of the fatigue data and a higher scatter factor is used to allow for this.

6.2 Scatter Factors

Scatter factors were derived from the product of four reliability factors (R_1 .. R_4 : see Table 4) following a procedure outlined in Reference (6).

	Reliability Factor
Accuracy of load spectrum: Wing	1.1 R_1
Tailplane	1.5
Cycle counting technique	1.03 R_2
Scatter in σ measurement: Inner wing	1.17 R_3
Outer wing and tailplane	2.00
Inherent scatter in fatigue performance	3.33 R_4

Factor R_1 is to compensate for variations in load spectra between sailplanes and has been taken as 1.1 for the wing and 1.5 for other areas following Maxwell (7). R_2 allows for variation between the cycle counting techniques and a factor of only 3% was found in the analysis carried out on a measured load sequence. R_3 allows for variability in stress per g and for the outer wing a factor of 2 has been adopted following Raithby (8). For other areas where measurements were obtained a 95% confidence interval for the recorded stress per g yields a difference in life of 17% giving a factor of 1.17.

The R_4 factor accounts for the scatter obtained where a number of specimens are tested and a value of 3.33 has been taken following Maxwell (7).

A product of the reliability factors gives for the wing:

$$SF(\text{inner wing}) = 1.1 \times 1.03 \times 1.17 \times 3.33 = 4.4$$

$$SF(\text{outer wing}) = 1.1 \times 1.03 \times 2.00 \times 3.33 = 7.5$$

and for the tailplane:

$$SF(\text{tailplane}) = 1.5 \times 1.03 \times 2.00 \times 3.33 = 10$$

These derived factors show good agreement with the guidelines of the Civil Aviation Authority and the Federal Aviation Administration, and relative to those values are probably on the conservative side for the tailplane and

outer wing where the in-flight stress per g has been measured rather than estimated by calculation.

6.3 Life Calculation

Final life calculations for each critical area are made by converting the maximum and minimum g values of the flight load spectra into stress quantities using the most representative stress per g, thus producing a stress spectrum (retaining the step-wise approximation to the continuous spectrum).

The steps in the stress spectra represent blocks of constant amplitude stress cycles, which is a simplified stress history for that area. The damage for each step in the stress spectrum is calculated by finding the endurance in cycles associated with the alternating and mean stress of the step and dividing the number of cycles occurring by that endurance. Summing the damages for each step then gives the total damage incurred per hour while operating under the stress spectrum used. This is the assumption of linear cumulative damage. If failure is then assumed to occur at a total damage of unity (in those areas tested during the manufacturers full scale fatigue test, relevant S-N data have been adjusted to predict the test result so this assumption is valid - in other areas it is covered by the increased scatter factor), the life in hours is found by taking the inverse of the damage. The lives for all areas so calculated are shown in Table 5 where the appropriate scatter factor has been applied. Allowance was made in these calculations for the lower stresses found during the tow launch and upon application of wing flaps during landing.

Area	Fatigue Data				
	Ref [4]	E.02.01	Ref [5]	E.05.01	E.05.05
1	-	15,300	15,900	-	-
2	-	-	-	15,100	-
3	-	-	-	-	17,100
4	-	103,500	-	-	-
5	23,000	-	-	-	-

7. Life Extension by Inspection

The program is continuing to establish inspection intervals for the safe detection of growing cracks and it is hoped this will enable a considerable extension in life to be achieved.

The DEFSTAN specification as used in the UK military specification is considered to be the most comprehensive specification available. A fracture mechanics approach using fracture toughness and crack propagation data published in the literature are used with adequate safety factors to avoid substantiating tests since there is a fleet of only six sailplanes involved.

As an example, cracks emanating from a hole in the spar attaching to the root rib are taken to illustrate the approach. Cracks from both sides of the hole are considered as a matter of conservatism. For this configuration the 80% ultimate design strength condition imposed by the DEFSTAN gives a corresponding stress of approximately 210

MPa and the tolerable crack length is about 19 mm (total crack length).

The Forman crack propagation law for 2024-T3 sheet (5) is given:

$$\frac{da}{dN} = \frac{7.13 \times 10^{-6} \times \Delta K^{2.7}}{(1-R) \times 71.3 - \Delta K}$$

The change in stress intensity factor under fluctuating stress is given by:

$$\Delta K = \Delta \sigma \sqrt{(\pi \times a)} \times \lambda \times \beta$$

where λ is a finite width correction factor and β is the Bowie correction factor for the hole with a crack present. A crack propagation curve has been calculated for this case and is shown for the purpose of example in Figure 12. The analysis is proceeding and will be applied to all of the most critical fatigue areas.

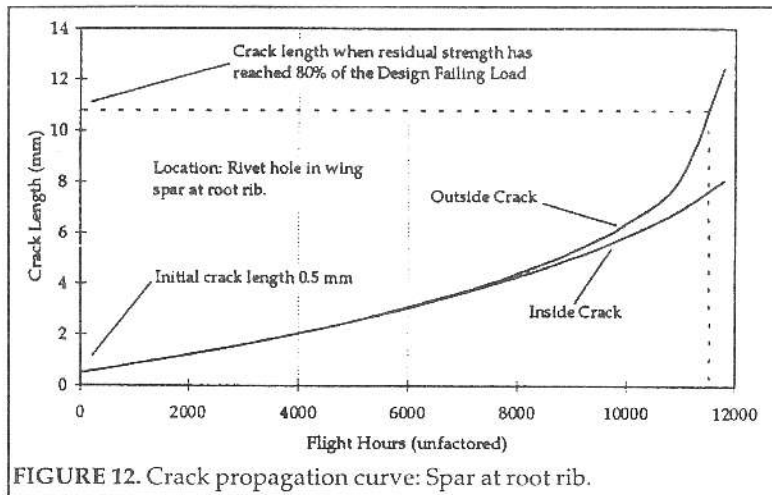


FIGURE 12. Crack propagation curve: Spar at root rib.

8. Conclusion

It is concluded that all fatigue prone areas of the airframe have been identified and safe fatigue lives for the GCV operations have been derived on a duly conservative basis. Although conservative the fatigue lives in the critical areas are all similar indicating a sound fatigue design. The minimum of the calculated fatigue lives for each area is 15,100 hours (with no aerobatic restrictions) for the spar to lug joint which is therefore taken as the minimum safe life

for the structure. All calculated safe lives are specific to the GCV fleet of IS28B2s and typical GCV operations with aero-tow launch methods only.

9. References

- (1) P. Liszka, Comp., *Establishing the IS28B2 Glider Safe Life*. M.I.C.M. - C.N.I.A.R. Intreprinderea De Constructii Aeronautice, 2200, Brasov, 1982.
- (2) G. P. Esson and C. A. Patching, "Fatigue Life Considerations for Gliders Operated in Australia", *Technical Soaring*, Vol. VI, No. 3:10-16.
- (3) A. O. Payne, "Determination of the Fatigue Resistance of Aircraft Wings by Full Scale Testing", *Full Scale Fatigue Testing of Aircraft Structures*. J. Plantema and J. Schijve eds. Pergamon Press: London, 1961: 76-132.
- (4) R. Hangartner, *Correlation of Fatigue Data for Aluminum Aircraft Wing and Tail Structures*. Report R-582, National Aeronautical Establishment, Ottawa, Canada, December 1974.
- (5) L. Schwarmann, *Material Data of High-Strength Aluminum Alloys for Durability Evaluation of Structures: Fatigue Strength, Crack Propagation, Fracture Toughness*. 2nd ed. Dusseldorf: Aluminum-Verlag, 1988.
- (6) A. F. Selikhov, V. L. Raikher, G. I. Nesterenko, V. G. Leibov, "The Methodology of, and the Experience in Providing the Structural Integrity of Aging Aircraft", *International Conference on Aircraft Damage Assessment and Repair: Proceedings*. Melbourne, 26-28 August, 1991:176-180.
- (7) R. D. J. Maxwell, "The Practical Implementation of Fatigue Requirements to Military Aircraft and Helicopters in the United Kingdom", *Proceedings of the 6th ICAF Symposium*, Miami Beach, May 1971.
- (8) K. D. Raithby, "A Comparison of Predicted and Achieved Fatigue Lives of Aircraft Structures", *Fatigue of Aircraft Structures*. W. Barrois and E. L. Ripley eds. ICAF Symp., Paris 1961: Pergamon Press, 1963: 249-261.
- (9) J. Schijve, "The Analysis of Random Load - Time Histories with Relation to Fatigue Tests and Life Calculations", *Fatigue of Aircraft Structures*. W. Barrois and E. L. Ripley eds. ICAF Symp., Paris 1961: Pergamon Press, 1963.
- (10) C. A. Patching, "Establishing the Structural Integrity of Aging Gliders", *Technical Soaring*, Vol. 1, No. 2, October 1971:17-25.